

# A Remote Sensing Approach for Measuring Climatic Change Effects on Snow Cover Dynamics

Francesco Parizia <sup>1,2</sup>, Samuele De Petris <sup>2</sup>, Luigi Perotti <sup>2,3</sup>, Marco Giardino <sup>3,4</sup>, Enrico Borgogno-Mondino <sup>2</sup>

5 <sup>1</sup> Department of Civil, Building and Environmental Engineering, Università di Roma “La Sapienza”, Via Eudossiana 18, Roma, 00184, Italy

<sup>2</sup> Università degli Studi di Torino, Department of Agricultural, Forest and Food Sciences, Largo Paolo Braccini 2, Grugliasco (TO), 10095, Italy

<sup>3</sup> Italian Glaciological Committee, Corso Massimo D’Azeglio 42, Torino (TO), 10125, Italy

10 <sup>4</sup> Università degli Studi di Torino, Department of Earth Sciences, Via Valperga Caluso 35, Torino (TO), 10125, Italy

*Correspondence to:* Luigi Perotti (luigi.perotti@unito.it)

**Abstract.** Climate change (CC) is significantly impacting the snow cover of the European Alps, compromising hydrological cycles, water stock for agricultural and civil supply, winter tourism. This study investigates Snow Cover Changes (SCC) in the Western Italian Alps (Piemonte and Valle d’Aosta regions) from 2000 to 2023, using MODIS satellite data. In particular, MOD10A1 images were processed in Google Earth Engine to derive daily snow cover, integral snow cover area (iSCA), snow persistence (SP), and mean daily snowed area (MDSA). Ground data from 96 snowmeter stations were used to validate the satellite-derived SP. The analysis of SCC was performed by quantifying long-term trends of MDSA at-the-pixel-level. The normalized trend ( $nT$ ) index represents the percentage change rate in snow-covered area per yearly mean snow event. It was mapped showing different spatial patterns of SCC in the study area. Results reveal an altitudinal gradient in  $nT$ , with the higher snow cover reduction occurring in lowland and within main valley areas, reaching -5% below 1000m a.s.l. and -1.8% between 1000-1500 m a.s.l. These findings highlight the vulnerability of snow resources due to CC, impacting water availability, winter sports, and regional economies. This study can support adaptation strategies and sustainable resource management in the Western Alps by mapping critical areas where CC effects on snow must be mitigated.

## 1 Introduction

25 Snow plays a crucial role both in environmental and economic sectors of the Alpine region, such as in the areas of Piemonte and Valle d’Aosta Regions. It has implications either in the economy, as a defining feature of the winter landscape, attracting tourists and sports people or for the hydrological cycle (Steiger et al., 2019; Sturm et al., 2017). Snow provides abundant quantities of water stocked during the winter and slowly released in spring and summer, creating an important supply for the Alpine valleys and communities. In the last few years, Climate Change (CC) is reshaping this dynamic: due to the rising 30 temperatures, snowfalls are reducing in lowlands and middle mountains, altering melt patterns (Intergovernmental Panel on Climate Change (IPCC), 2022). The climatic emergency poses significant challenges for water management in the region,

where water supplies, both in industrial/agricultural and domestic use, depend heavily on the seasonal snowpack, impacting the environment and the economy.

Since the early 1900s, many climatic series studies demonstrate how the climate is changing in the Alpine Region with regards to Piemonte and Valle d'Aosta and how the precipitation (especially the snow) is changing too. In 1964 the Italian Glaciological Committee (CGI) published a bulletin (Comitato Glaciologico Italiano, 1964) in which a snow cover map (1959-1960) was disseminated in order to represent the day of snow persistence on the ground. This product was very interesting at the time, to study and design the reservoirs that were being built. In (Cati, 1981) dataset on snow cover were shown for the period 1921-1950 and it was written that prof. Gazzolo and prof. Pinna (Gazzolo, 1973; Gazzolo and Pinna, 1973; Pinna, 1973) analyzed that at that time the mean temperature and the related snowfalls were decreased, compared to the previous years of the late 1800s. In 1971, the Institute of Alpine Geography published a volume (Ogliaro, 1971) on the changes of the snow, in terms of permanence and frequency in the thirty years between 1929 and 1958. They observed that the snow persistence registered a common decrease in all the alpine sectors comparing the second 15 years to the firsts (1944-1958 compared to 1929-1943). The variations of the snow persistence were in terms of 20-35 days lost. Also the days of snow precipitation changed, with values of 7-10 days of precipitation lost by the second 15 years compared to the firsts. In 2013 Arpa Piemonte, regional environmental agency, published a report (Faletto et al., 2013) on the snow changes in Piemonte's Alps for the period 1961-2010. The report underlined how the snow cover and the snow falls were in continuous change. Authors analyzed the snow persistence changes with results of a mean decrease of -0.5 days/season of persistence lost over the entire period of 50 years, with peak values of -1.19 days/season. Regarding the precipitations, the values were comparable: a mean value of -0.1 days/season with peak values of 0.28 days/season. In the last few years, different researches were published about Snow Cover Changes (SCC) in mountains area using multispectral satellite datasets (Fugazza et al., 2021; Maskey et al., 2011; Melón-Nava, 2024; Riggs et al., 2022; Saavedra et al., 2018). Moreover, many remote sensed technologies have been used in the years to perform studies on snow evolution: Multispectral studies, SAR analysis and also the creation of new Spectral Index for a better detection of the snow (Arreola-Esquivel et al., 2021; Corazza, 2024; Poussin et al., 2025; Tsai et al., 2019).

The aim of this paper is to reconstruct the evolution of snow cover, from 2000 to 2023, using multispectral remote sensing technologies (Moderate-resolution Imaging Spectroradiometer - MODIS). In particular our goal is not to track snow phenology but to quantify the accumulated loss of intensity of snow cover for a single mean snow event. This paper is not intended to replace statistical trend methods (such as Mann-Kendall (Mann, 1945) or Sen's slope (Sen, 1968)), but rather to offer a complementary, easily interpretable, and spatially explicit measure. The main goal is to provide a new metric, which differs from analyses focused on phenological metrics (Start Of Season/End Of Season): this metric will allow a deeper understanding of how the intensity of snow covering, of a mean snow event, has evolved annually. This product will reflect the evolution of this trend within each individual pixel and it is inherently comparable across the entire study area. Consequently, the interpretation of this spatial result is not directly affected by the confounding influence of elevation or other environmental

65 drivers, when assessing the rate of change within that specific location. We believe that parameterizing this behavior is of paramount importance for regional impact assessment.

## 2 Materials and Methods

### 2.1 Area of interest

70 Area of Interest (AOI) is the Italian Western Alps within the regions of Piemonte and Valle d'Aosta. The morphological setting of the AOI is quite complex (Fig. 1): most of the territory is mountainous and hilly and the lowlands are closely linked to the dynamics of the higher areas.

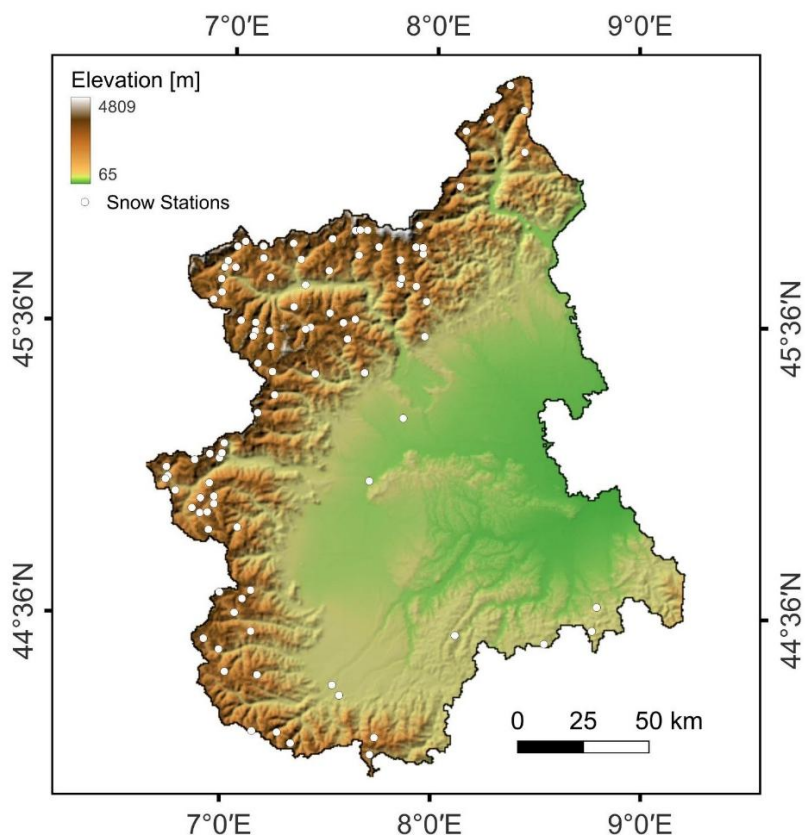


**Figure 1:** AOI, its morphological complexity and the distribution of the different topographic areas. The white dots represent the snowmeter stations of Arpa Piemonte and Arpa Valle d'Aosta used as ground truth.

75 Due to the AOI geological/geomorphological asset, the water supply of the lowlands is directly correlated with the water runoff in mountainous areas. In fact, the snow cover offers a natural stock of fresh water during the winter months, and its ecosystem service is necessary to the adequate water recharge of canals and aquifers mainly on the lowlands.

## 2.2 Data collection

### 2.2.1 MODIS and Elevation data

MODIS is a satellite mission that provides multispectral imagery with a temporal resolution of 1 day from 2000. In this work, the product MOD10A1.061 Terra was selected and pre-processed in Google Earth Engine (GEE) platform making it possible to monitor the daily evolution of the snow cover at a small scale. In particular, MOD10A1 provides daily snow cover data (in percentage) with a geometric resolution of 500 m (Hall et al., 2002; Liu et al., 2020; Salomonson and Appel, 2004) representing the fraction of the pixel covered by snow. About 8400 images were selected and processed directly in GEE (Gorelick et al., 2017) covering the sensing period between 1st October 2000 and 30th September 2023 over AOI.

This collection product was selected because it was the only long-term MODIS snow dataset (2000-2023) fully available in the GEE catalog. Gap-filled products such as MOD10A1F/MYD10A1F were not accessible in GEE. Moreover, the use of GEE was essential to perform advanced, large-area and dense time-series analyses that would not have been computationally feasible outside the platform.

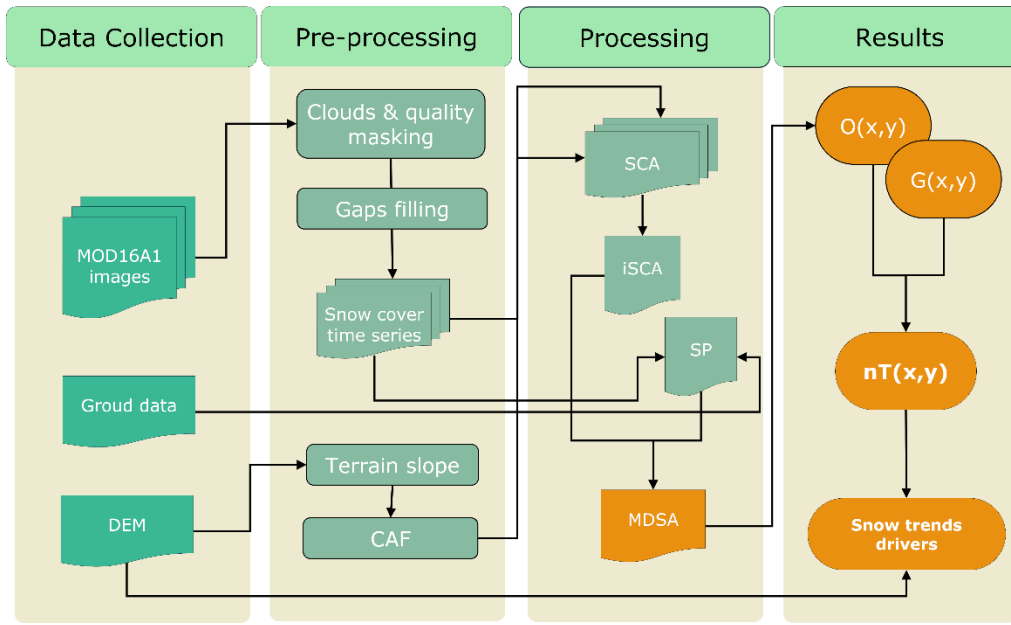
In order to analyze and correct snow cover data in respect to altitude and terrain slope, the Copernicus DEM GLO-30 (Trevisani et al., 2022) was collected and processed in GEE. Copernicus DEM GLO-30 is a raster layer updated in 2015 that maps altitude data with a geometric resolution of 30 m.

### 2.2.2 Ground data

The necessity for the ground truth emerged because of the fundamental validation process. The AOI is varied: wide lowlands, hilly areas and mountains of variable elevation, up to an altitude of 4805 m a.s.l. (Mont Blanc). We collected data from snowmeter stations inside the networks of stations of Arpa Piemonte and Arpa Valle d'Aosta (Banca dati storica - Arpa Piemonte, 2025; Dataview - Arpa VdA, 2025) covering the entire AOI. The two networks together have more than one hundred stations well distributed throughout the entire territory. To perform this study, it was decided to use 96 stations, all the stations that have dataset for the analyzed period (also partially). The dataset was acquired from the websites of each agency, according to the period of analysis: 1st October 2000 to 30th September 2023. The distribution of the station is visible in Figure 1.

## 2.3 Data processing

The workflow adopted in this study is reported in Figure 2 (1) Data collection step involves collecting and preparing the MOD16A1, terrain data and ground reference samples required for calibrating and testing derived snow products (2) Data pre-processing step focuses on filtering, masking, and computing snow cover time series and terrain calibration. (3) Processing steps include correcting snow cover area by using DEM data and performing yearly aggregation. (4) Results steps are aimed at statistically quantify snow cover trends and assessing which environmental drivers affect them. Methodological details are described in the next sections.



110 **Figure 2: Workflow adopted. Arrows represent the data flow from input data (light green) through methodological steps (in dark green) to the obtained results (in orange).**

### 2.3.1 Mapping Snow Cover Area, Persistence and daily snowed area

115 Daily snow cover was derived from the MODIS MOD10A1 Collection 6.1 product, which provides fractional snow cover (NDSI Snow Cover, %) at a nominal spatial resolution of 500 m (Hall and Riggs, 2016). The analysis was conducted within Google Earth Engine (GEE). The area of interest (AOI) was defined by merging the administrative boundaries of Valle d'Aosta and Piemonte regions. A digital elevation model (DEM) was obtained from the Copernicus GLO-30 dataset (30 m spatial resolution). The DEM was mosaicked and clipped to the AOI and subsequently reprojected to the native MODIS sinusoidal grid using the projection information extracted from the MOD10A1 NDSI Snow Cover band. The DEM was resampled to 500 m using mean aggregation to ensure spatial consistency with the MODIS data. Terrain slope  $\theta_i$  was computed from the resampled DEM and used to correct the nominal MODIS pixel area ( $A_p = 500 \times 500m^2$ ) for topographic distortion. A correction area factor (CAF) was defined in Equation (1):

$$CAF_i = \frac{A_p}{\cos(\theta_i)} \quad (1)$$

where  $\theta_i$  is the local terrain slope at pixel  $i$ . The CAF was expressed in hectares and applied uniformly to all MODIS observations.

125 Missing values in the MODIS daily snow time series, mostly caused by cloud contamination, were reconstructed using a linear interpolation approach. Although snow cover can vary rapidly, linear interpolation provides a conservative and well-controlled method that relies exclusively on the closest valid observations, avoiding the introduction of artificial temporal patterns. More

130 complex gap-filling techniques (e.g., splines, LOESS, Savitzky–Golay) tend to oversmooth or generate oscillatory behaviour, especially in heterogeneous mountainous regions. These methods may also propagate unrealistic transitions across short gaps, producing artefacts that can bias trend analyses. Given the large spatial extent and high temporal density of the dataset, linear interpolation offers the best balance between computational robustness, reproducibility, and physical consistency. This method ensures that derived metrics remain comparable and stable across the study area.

135 Subsequently, quality control was performed using both quality layers provided in the MOD10A1 product. First, the NDSI\_Snow\_Cover\_Basic\_QA layer was used to retain only pixels classified as Best (0) or Good (1) quality. Second, the NDSI\_Snow\_Cover\_Algorithm\_Flags\_QA layer was used to further exclude pixels flagged as inland water (bit 0), visible screen failure (bit 1), NDSI screen failure (bit 2), or solar zenith screen failure (bit 7). Only pixels for which all selected bits were equal to zero were retained. This combined masking strategy ensured that only high-quality, physically reliable snow cover observations were used. Clouds and quality masking introduced missing values in the daily snow cover time series. These gaps were filled using linear temporal interpolation within a  $\pm 30$ -day moving window. For each pixel  $i$  and missing observation at time  $t$  snow cover was reconstructed using the closest valid observations before ( $t_1$ ) and after ( $t_2$ ) the gap, as  
 140 following Eq (2):

$$NDSI_i = NDSI_i(t_1) + \frac{t-t_1}{t_2-t_1} [NDSI_i(t_2) - NDSI_i(t_1)] \quad (2)$$

This approach relies exclusively on observed values and avoids the introduction of artificial temporal patterns, providing a conservative and reproducible gap-filling strategy suitable for large mountainous regions. For each  $i$ -th pixel and acquisition time  $t$ , the snow-covered area (SCA, ha) was computed as follow (3):

$$145 \quad SCA_{i,t} = \frac{NDSI_{i,t}}{100} \times CAF_i \quad (3)$$

Where  $NDSI_{i,t}$  is the fractional snow cover expressed in percentage. Daily SCA maps thus represent the effective snow-covered surface accounting for terrain-induced pixel area distortion. Consequently, snow persistence was computed for each hydrological year (1 October–30 September). A binary snow mask  $B_{i,t}$  was generated for each daily observation as shown in Eq (4):

$$150 \quad B_{i,t} = \begin{cases} 1, & \text{if } NDSI_{i,t} > 0, \\ 0, & \text{otherwise} \end{cases} \quad (4)$$

Annual snow persistence (SP, days) was obtained by summing the binary mask over time is represented in Eq (5):

$$SP_i^{(y)} = \sum_{t=1}^{N_y} B_{i,t} \times \Delta t_t \quad (5)$$

Where  $N_y$  is the number of observations in  $y$ -th hydrological year and  $\Delta t_t$  is the temporal interval in days between consecutive acquisitions. Furthermore, the integrated snow-covered area (iSCA) for each hydrological year was computed as reported in  
 155 Eq. (6):

$$iSCA_i^{(y)} = \sum_{t=1}^{N_y} SCA_{i,t} \times \Delta t_t \quad (6)$$

Finally, the mean daily snow-covered area (MDSA, ha) was defined as the ratio between integrated snow-covered area and snow persistence. Eq (7):

$$MDSA_i^{(y)} = \frac{iSCA_i^{(y)}}{SP_i^{(y)}} \quad (7)$$

160 This metric represents the average snow-covered area during snow-covered days and is independent of the length of the snow season, allowing robust inter-annual comparison of snow accumulation intensity at the pixel scale.

### 2.3.2 Snow Persistence Validation

The environmental preservation service, which in the territories of Piemonte and Valle d'Aosta is carried out by the Arpa agencies, made available, free of charge, the nivometric stations datasets with a time series of nivological metrics, starting  
 165 from the mid-1900s. These data were used as validation of the working method used for this study. In fact, we compared the single pixel of SP product with the corresponding daily snow presence derived by the snowmeter stations. The process was performed on a yearly basis, in order to obtain a continuous validation dataset for the long-term monitoring period. In this way, it was possible to obtain a curve describing, annually, the amount of days of snow presence on the ground from either station data and data obtained from satellite observation. This process led to a temporal comparison of the amount of days of snow  
 170 persistence on the ground in order to be able to validate the values obtained from the SP product.

### 2.3.3 Snow Cover Trends Quantification

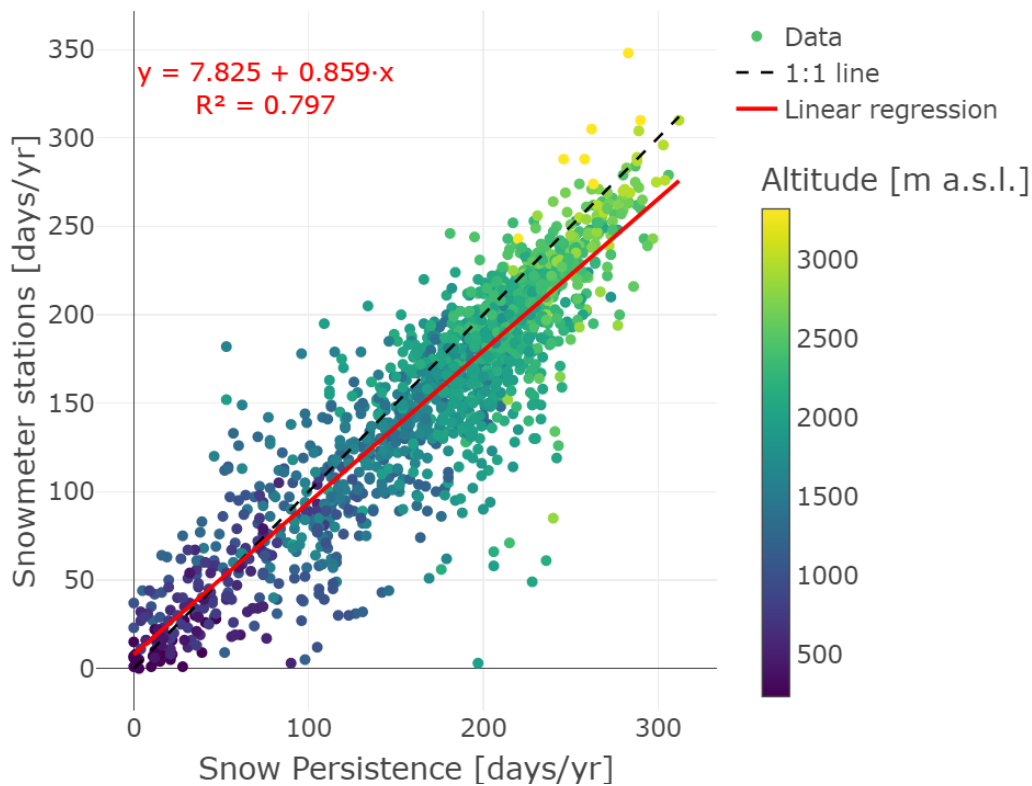
Once MDSA multiannual stack was downloaded from GEE, a self-develop routine was implemented in the R vs 4.1.1 environment in order to analyze at-the-pixel-level the long-term SCC in AOI. In particular, a linear regression was locally fitted involving 23 MDSA values as the dependent variable and the year as the independent one. The slope (Gain) and intercept  
 175 (Offset) parameters derived by ordinary least squares method (OLS) were mapped into 2 new layers called G(x,y) and O(x,y) having the 500 m of geometric resolution. G(x,y) maps the local increment or decrement of MDSA along the considered period. This value shows the multi-annual trend of a given area to change the daily snow cover. To assess if this trend is significantly different from 0 (i.e., flat trend or not significant changes), a two-tailed t-test (Koch, 1999) on slope parameter from OLS was performed involving 22 degree-of freedoms and a significance level of 95%. All G(x,y) pixels not significant  
 180 were masked out. Moreover, the determination coefficient of linear regression was also mapped into a new layer called R2(x,y). The latter represents how the linear trend assumption fits the data. Since some areas in AOI may exhibit a quadratic or (high order polynomial) temporal behavior of MDSA, all pixels having  $R2(x,y) < 0.5$  were masked out. This removal allows to guarantee that remaining local trends show linear-like behavior in the considered period making it possible to easily quantify the SCC and future forecasting.

185 Finally,  $G(x,y)$  was divided by  $O(x,y)$  in order to create a new layer called normalized trend -  $nT(x,y)$ . The latter maps the change rate in respect to the year 2000 assumed as reference. This normalization allows to properly compare areas having different environmental starting conditions (e.g., mountain areas vs lowland ones). In fact,  $nT(x,y)$  represents changes in snow covered area in a single average snow event. Using the altitude classification according to Kapos (Kapos et al., 2000) the  $nT(x,y)$  map was divided in 6 groups according to an altitudinal gradient. The Kolmogorov-Smirnov test (KS) (Pratt and  
190 Gibbons, 1981) was adopted for assessing the differences among  $nT$  values distributions and exploring how altitude can be a driver of SCC in the considered period.

### 3 Results

#### 3.1 Snow Persistence Validation

The validation process resulted in a good correlation between ground and satellite datasets (Fig. 2).



195

**Figure 3: Days of snow persistence calculated by satellite product and ground stations represented in a scatter plot. Dots' colors represent the altitude of the investigated station/pixel. Red line represents the linear regression.**

Despite the important geometric difference between the two datasets (500 m vs single spot), the annual amount of snow persistence was very close. We obtained a R2 of 0.8 and a MAE of 20.4. The presence of a minimal offset (Fig. 2) is caused

200 by the geometric difference of the datasets in question: the punctual dataset compared to a 500 m pixel. In fact, in Fig. 4A we can see how the Antrona station, placed at an elevation of 1500 m a.s.l., presents an almost complete overlap of the curves. While in Fig. 4B in the Entracque - Chiotas station, placed at an altitude of 1970 m a.s.l., we can see how the trend of the satellite curve is flat, precisely because of the location of the weather station (above a dam placed on the threshold of a glacial cirque). Furthermore, as is clearly visible in Figure 3, the clustering of data points around 200 days/year causes the elevation of the offset compared to the points around 50 days/year, which closely follow the 1:1 line. This offset is caused by the mean elevation of the stations of around 1783 m a.s.l. and the median of 1905 m a.s.l. This elevation difference increases the impact of the topographic effect in the comparison between point measurement to the 500m pixel data. This resolution can carry a significant elevation range in mountainous areas. This bias introduces a constant error in the observation and comparison. This error leads to the overestimation of snow presence in mountain areas by the satellite product compared to the ground truth data (Fig. 4B).

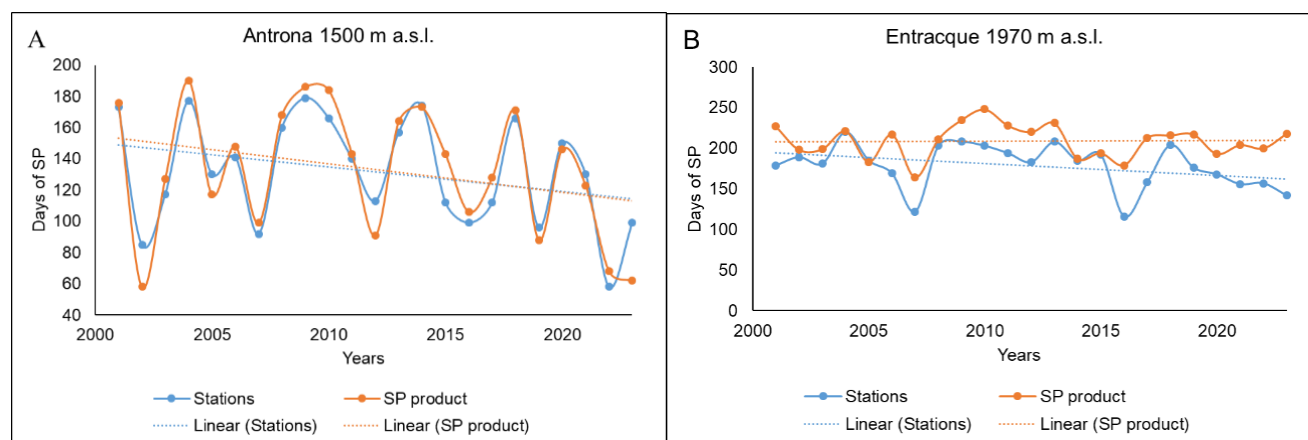
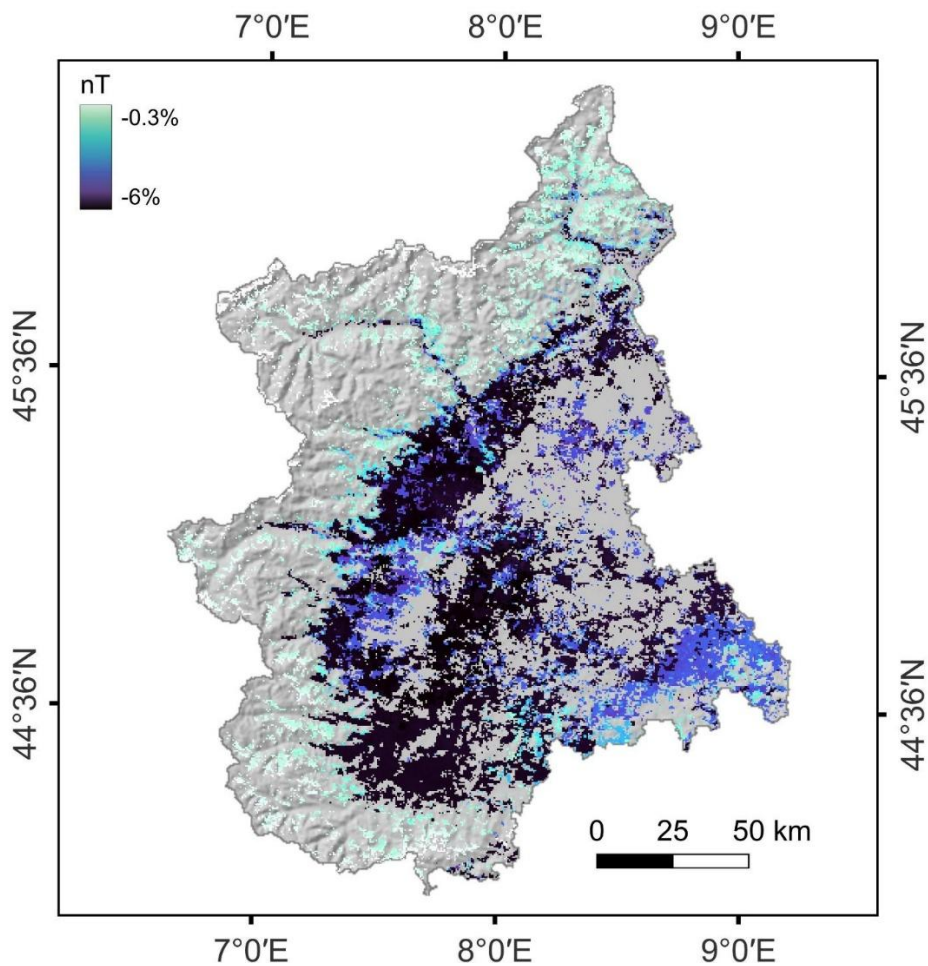


**Figure 4: yearly snow persistence comparing SP measure calculated from MODIS (orange) and ground snowmeter station (blue). A) Antrona station B) Entracque - Chiotas station. In B the satellite values (orange) are higher than the station ones (blue) underlighting showing a typical case of overestimation of snow presence.**

### 215 3.2 Snow Trends Quantification

As introduced in 2.3.1. and 2.3.3.  $nT$  represents a spatial product in which it is possible to assess how snow cover changed from 2000 to 2023 at the Italian Western Alps territory level. The  $nT$  product represents the percentage change yearly rate in snow covered area (at pixel level) for a single mean event in respect to  $t_0$  conditions (in the specific case 2000). By normalizing the series with respect to the model intercept we express the gain as a relative change rather than as an absolute value. This operation removes site-specific baseline effects, allowing a consistent and dimensionless comparison of trends across spatially heterogeneous locations. The year 2000 ( $t_0$ ) is the mathematical origin of the time variable in our model, and serves as a standardized reference point for comparing the relative magnitude of temporal changes across sites. This modeling approach provides a direct and interpretable framework for quantifying and comparing temporal trends across heterogeneous spatial domains. In Fig. 5 it is possible to observe the distribution of the changes in AOI.

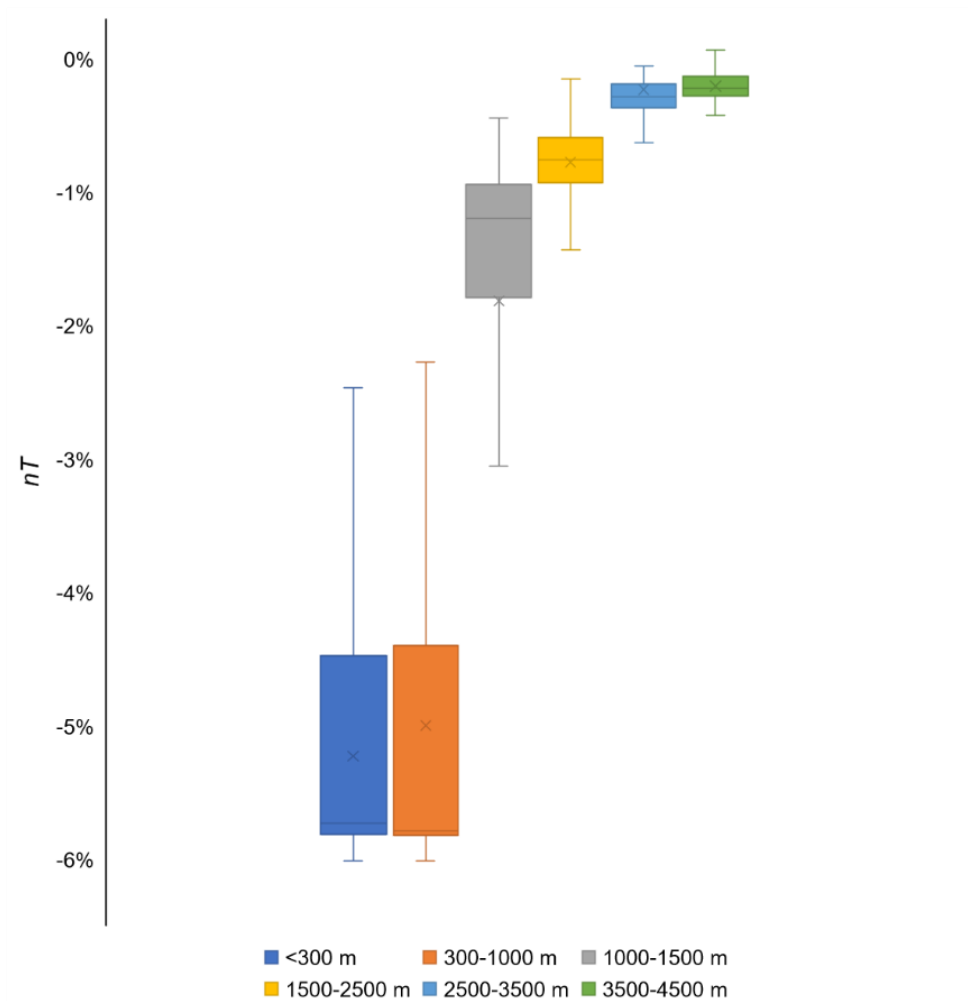


225

**Figure 5: Spatial representation of  $nT$ , strongly-negative values are related to low altitude areas, instead of less negative values, related to high altitude areas.**

Figure 5 shows  $nT$  values in AOI, some areas are not covered because of the masked sectors (as reported in chapter 2.3.3.) that are about 6% of the total pixel for the not significant gain and 58% for the low  $R^2(x,y)$  values. Analyzing figure 5, there is a significant trend in the spatial distribution of the obtained values. In fact, the most suffering areas are the ones in the lowlands and main valleys (low altitude sectors in fig. 1) evidenced by the dark blue colors. This impact seems to reduce moving upward in altitude. The altitudinal trend is well represented in figure 6.

230



235 **Figure 6:**  $nT$  in relation to the altitude of the AOI. The values of the altitude reported in meters are in m a.s.l. The altitude classification is taken from (Kapos et al., 2000). The boxes are drawn from 25th to 75th percentile with a horizontal line drawn inside it to denote the median and a cross to represent the mean of the data. The whiskers are drawn from the 5th to the 95th percentile.

Figure 6 shows the  $nT$  values distributions per altitudinal groups. It is worth noting how pixels with high altitude show in general lower  $nT$  values. In contrast, pixels on lowland groups show in higher  $nT$  supporting the hypothesis of an altitudinal  
 240 gradient of  $nT$  values with the following interpretative key: lowland areas show in general significant negative trends than high mountain ones. The latter have quite flat trends tending to 0. KS test results (Table 1) support this hypothesis denoting significance differences among altitudinal groups.

Table 1: Significance of boxplot in figure 6

p-value\ D	<300 m	300-1000 m	1000-1500 m	1500-2500 m	2500-3500 m	3500-4500 m
<300 m	-	0.18	0.817	0.989	0.999	0.999
300-1000 m	p < 0.001	-	0.718	0.943	0.996	0.998
1000-1500 m	p < 0.001	p < 0.001	-	0.52	0.961	0.996
1500-2500 m	p < 0.001	p < 0.001	p < 0.001	-	0.824	0.944
2500-3500 m	p < 0.001	p < 0.001	p < 0.001	p < 0.001	-	0.31
3500-4500 m	p < 0.001	p < 0.001	p < 0.001	p < 0.001	p < 0.001	-

#### 4 Discussion and Conclusion

245 The long-term assessment of snow-cover dynamics in alpine regions requires satellite observations that are both temporally  
continuous and capable of capturing the full intra-seasonal variability of snow processes. In this context, MODIS stands out  
as the only Earth observation mission providing a daily and uninterrupted multi-decadal record, which is essential for deriving  
temporally integrated metrics such as snow persistence, snow-cover duration, and long-term trends. Although higher-resolution  
missions such as Landsat and Sentinel-2 offer improved spatial detail, their substantially lower revisit frequencies (16 days for  
250 Landsat; 5–10 days for Sentinel-2) combined with persistent cloud cover in mountain environments lead to highly  
discontinuous time series (Gascoïn et al., 2015; Parajka and Blöschl, 2008). These limitations introduce major uncertainties  
when estimating metrics reliant on daily observations, particularly the number of snow-covered days. Furthermore, neither  
Landsat nor Sentinel currently provides a temporally complete archive comparable to the 23-year MODIS record used in this  
study. For these reasons, MOD10A1 remains the only dataset capable of supporting long-term, high-frequency analyses of  
255 alpine snow climatology, forming a robust foundation for interpreting the time-space patterns.

Results from this study can be used for highlighting the effects of climate warming within the Italian Western Alps due to SCC  
in the last two decades. In fact,  $nT$  synthesizes the percentage variation of snow cover intensity by looking at a single yearly  
mean snow event. In literature, there are several works that observe phenological changes from satellites: seasonality,  
persistence, first snowfall (Fugazza et al., 2021; Maskey et al., 2011; Notarnicola, 2020). By introducing the  $nT$  concept, we  
260 observe the intensity and impact of changes affecting snow cover, on a regional scale, beyond the phenological indexes.  $nT$   
value makes it possible to summarize the intensity of SCC and enhances the understanding of its evolutionary trends. From  
the Earth Observation point of view,  $nT$  is a good metric to properly compare pixels from different geographic areas. Therefore,  
it allows to spatialize and describe the effect of the CC in terms of snow cover.  $nT$  is independent from the changes of

seasonality of the snow (i.e., from the length of snow period). It enhances interpretation of environmental changes through the time, summarizing the changing rate (i.e.,  $G(x,y)$ ) and the starting conditions (i.e.,  $O(x,y)$ ).

Application of  $nT$  within the AOI (Figure 5) highlights clear geo-environmental patterns in the spatial distribution of SCC: the most negative values corresponds to the Cuneo's lowlands, Po Plain and to the main valleys such as Susa Valley, Aosta Valley and Ossola Valley. Then values increase by altimetric position but not homogeneously. With respect to this, further constraints are latitudinal and geomorphological position (e.g. internal or external position in the mountain belt, proximity to the valleys, exposure, ...). The most negative values show that the negative trends lead to a complete absence of snow cover. The dark areas in Figure 5 are showing no more whitening snow events for the last few years. The geo-environmental patterns are well described in Figure 6. In fact, results of altitudinal classification within the AOI (Fig. 6) shows the extreme impact of  $nT$  at low altitudes (below 1000 m a.s.l.) quantified in -5% per year. In addition, other two areas are strong affected by CC: 1000-1500 m a.s.l. (-1.8%) and 1500-2500 m a.s.l. (-0.7%). As mentioned  $nT$  shows the changes in snow-whitened areas for a single yearly mean event. This represents that changes are indeed occurring at all elevations, but with greater intensity (in percentage terms, relative to its own mean starting value) at lower elevations. Observing the entire period of  $nT$  study, below 1000 m a.s.l. the whitening power of a mean snow event has mostly disappeared and between 1000-1500 m a.s.l. are reduced by more than 40%.

The observed snow loss at high altitudes, even if it is known that at that elevation the temperature is still below zero degrees, is primarily attributable to two main reasons. Firstly, the increasing air temperatures are frequently driving the zero-degree isotherm to elevations well above the highest peaks in the study area ( $\approx 4500$  m a.s.l.). This results in non-snow precipitation and extreme melting of the snow during these events. Then, the significant reduction in the extent of perennial snowfields within the study region is also captured by the MODIS snow cover product. Areas that historically maintained permanent snow (e.g., above 3500 m a.s.l.) have experienced substantial ablation and retreat over the 23-year period. This reduction in historically persistent snow contributes to the overall negative  $nT$  values, even if the effect is small over a two-decade trend analysis. Therefore, while temperatures remain below zero for much of the year at high altitudes, the increasing frequency of warm-air intrusions and the substantial reduction of permanent snow explain the overall negative, yet often minimal, trends observed in Figures 5 and 6.

The evolution process, evidenced by  $nT$  in Figure 5, shows that the areas whitened by a single snow event are decreasing. This result offered by the application of our method is a clear representation of the freezing level is moving upward (in elevation) and the decreasing of snow precipitation. The potential snowfall is becoming almost zero at low altitudes (below 1000 m a.s.l.) and very weak in the mid-mountains (1000-1500 m a.s.l.).

Many studies (Avanzi, 2024; Avanzi et al., 2024; Berghald et al., 2025; Bozzoli et al., 2024; Matiu et al., 2021) observed that temperature and precipitation are changing in the AOI. In fact, it is reported that the precipitation are changing in terms intensity (Berghald et al., 2025) and temporal distribution but remaining almost the same for annual value. This effect of the climate emergency, related to the rising temperatures lead to the reduction of the snow season, especially for the areas below 2000 m (Matiu et al., 2021). As reported by Avanzi (Avanzi, 2024; Avanzi et al., 2024) the drought of the last years affected

most, the areas below 1500 m a.s.l. The evidence is underpinned also by  $nT$ . As shown in Figure 6, the more suffering areas were the ones below 1500 m a.s.l., in which the trend is significantly negative. Same negative trend is reported, at a different observation scale, for whole Alpine Region (Bozzoli et al., 2024; Matiu et al., 2021). The spatial distribution of SCC, as highlighted by  $nT$  can be of significant value in terms of territorial and water management policies. Many considerations could be derived within the AOI based on our result, from various point of view: land use, tourism, and water resources.

This study presents some limits, the absence of a quantitative volumetric assessment of the observed changes. This limitation represents a significant future research challenge: quantifying snowpack volume necessitates the exploitation of spatiotemporal Snow Water Equivalent (SWE) data. Furthermore, a portion of the study area currently exhibits non-linear or undefined trends in the observed changes. Consequently, repeated temporal observations will be crucial to accurately discern and characterize the evolving dynamics within these specific sectors.

Nevertheless, the findings of this study offer strategic implications for Alpine communities, underscoring the critical importance of effective water resource management across industrial, agricultural, and public consumption sectors. Moreover, in light of the progressive snow cover reduction documented herein, it is imperative to critically evaluate the long-term sustainability of certain winter sports activities at elevations below 1500 m a.s.l.

Snow Cover in the Western Alps is undergoing changes that have significant repercussions on the whole sector. This study revealed, using MODIS satellite data, the effects of the Climate Changes (CC) in the Italian Western Alps, in terms of Snow Cover Changes (SCC) in the period 2000-2023. The herein introduced normalized trend ( $nT$ ) index quantifies these changes by expressing the annual mean change in snow-covered area. Our findings indicate that lowland and main valley areas have undergone the most substantial decrease, with  $nT$  values decreasing by up to -5% below 1000 m a.s.l. and about -1.8% in areas between 1000-1500 m a.s.l. These findings show the influence of CC on regional snow dynamics, with implications for water resource management. Especially, winter tourism is critically affected by the reduction of snow cover and many winter stations had to close in the last decades. **The long-term sustainability of various economic activities should be re-planned. Also, agriculture should take into consideration the reduction of snow cover as a long-term water supply for the lowlands aquifers to assess future climatic scenarios on water provision.**

### Competing interests

The authors declare that they have no conflict of interest.

### References

325 Banca dati storica - Arpa Piemonte:  
[https://www.arpa.piemonte.it/rischi\\_naturali/snippets\\_arpa\\_graphs/map\\_meteoweb/?rete=stazione\\_meteorologica,](https://www.arpa.piemonte.it/rischi_naturali/snippets_arpa_graphs/map_meteoweb/?rete=stazione_meteorologica) last  
access: 17 February 2025.

- Dataview - Arpa VdA: [https://presidi2.regione.vda.it/str\\_dataview](https://presidi2.regione.vda.it/str_dataview), last access: 17 February 2025.
- Arreola-Esquivel, M., Toxqui-Quitl, C., Delgadillo-Herrera, M., Padilla-Vivanco, A., Ortega-Mendoza, G., and Carbone, A.:  
330 Non-Binary Snow Index for Multi-Component Surfaces, *Remote Sens.*, 13, 2777, <https://doi.org/10.3390/rs13142777>, 2021.
- Avanzi, F.: La neve di oggi è l'acqua di domani: cosa ci ha insegnato la siccità del 2021-2024, *Nimbus*, 92, 26–35, 2024.
- Avanzi, F., Munerol, F., Milelli, M., Gabellani, S., Massari, C., Giroto, M., Cremonese, E., Galvagno, M., Bruno, G., Morra  
di Cella, U., Rossi, L., Altamura, M., and Ferraris, L.: Winter snow deficit was a harbinger of summer 2022 socio-hydrologic  
drought in the Po Basin, Italy, *Commun. Earth Environ.*, 5, 64, <https://doi.org/10.1038/s43247-024-01222-z>, 2024.
- 335 Berghald, S., Blanchet, J., Blanc, A., and Penot, D.: Climatology and trends of observed daily and hourly extreme precipitation  
in the French Alps, *EGU sphere*, 2025, 1–35, <https://doi.org/10.5194/egusphere-2025-3073>, 2025.
- Bozzoli, M., Crespi, A., Matiu, M., Majone, B., Giovannini, L., Zardi, D., Brugnara, Y., Bozzo, A., Berro, D. C., Mercalli, L.,  
and Bertoldi, G.: Long-term snowfall trends and variability in the Alps, *Int. J. Climatol.*, 44, 4571–4591,  
<https://doi.org/10.1002/joc.8597>, 2024.
- 340 Cati, L.: *Idrografia e idrologia del Po*, Ministero dei Lavori Pubblici, Servizio Idrografico, 1981.
- Comitato Glaciologico Italiano: *Bollettino del Comitato Glaciologico Italiano*, Comitato Glaciologico Italiano, Torino, 1964.
- Corazza, L.: *Imaging snow with SAR: state of the art and validation with ground-based data*, PhD Thesis, 2024.
- Faletto, M., Prola, M. C., Acquaotta, F., Fratianni, S., and Terzago, S.: *La Neve Sulle Alpi Piemontesi. Quadro conoscitivo  
aggiornato al cinquantennio 1961-2010*, Arpa Piemonte, 2013.
- 345 Fugazza, D., Manara, V., Senese, A., Diolaiuti, G., and Maugeri, M.: Snow Cover Variability in the Greater Alpine Region in  
the MODIS Era (2000–2019), *Remote Sens.*, 13, 2945, <https://doi.org/10.3390/rs13152945>, 2021.
- Gascoin, S., Hagolle, O., Huc, M., Jarlan, L., Dejoux, J.-F., Szczypta, C., Marti, R., and Sánchez, R.: A snow cover climatology  
for the Pyrenees from MODIS snow products, *Hydrol. Earth Syst. Sci.*, 19, 2337–2351, [https://doi.org/10.5194/hess-19-2337-](https://doi.org/10.5194/hess-19-2337-2015)  
2015, 2015.
- 350 Gazzolo, T.: *Le precipitazioni nevose in Italia*, in: *Atti della Tavola Rotonda sulla Geografia della Neve in Italia*, 1973.
- Gazzolo, T. and Pinna, M.: *La nevosità in Italia nel Quarantennio 1921-1960 (gelo, neve e manto nevoso)*, Istituto Poligrafico  
dello Stato, 1973.
- Gorelick, N., Hancher, M., Dixon, M., Ilyushchenko, S., Thau, D., and Moore, R.: Google Earth Engine: Planetary-scale  
geospatial analysis for everyone, *Remote Sens. Environ.*, 202, 18–27, 2017.
- 355 Hall, D. and Riggs, G.: MODIS/Terra Snow Cover Daily L3 Global 500m SIN Grid, Version 6,  
<https://doi.org/10.5067/MODIS/MOD10A1.006>, 2016.
- Hall, D. K., Riggs, G. A., Salomonson, V. V., DiGirolamo, N. E., and Bayr, K. J.: MODIS snow-cover products, *Remote Sens.  
Environ.*, 83, 181–194, [https://doi.org/10.1016/S0034-4257\(02\)00095-0](https://doi.org/10.1016/S0034-4257(02)00095-0), 2002.
- Intergovernmental Panel on Climate Change (IPCC) (Ed.): *High Mountain Areas*, in: *The Ocean and Cryosphere in a Changing  
360 Climate: Special Report of the Intergovernmental Panel on Climate Change*, Cambridge University Press, Cambridge, 131–  
202, <https://doi.org/10.1017/9781009157964.004>, 2022.

- Koch, K.-R.: *Parameter Estimation and Hypothesis Testing in Linear Models*, Springer, Berlin, Heidelberg, <https://doi.org/10.1007/978-3-662-03976-2>, 1999.
- Liu, C., Li, Z., Zhang, P., Zeng, J., Gao, S., and Zheng, Z.: An Assessment and Error Analysis of MOD10A1 Snow Product Using Landsat and Ground Observations Over China During 2000–2016, *IEEE J. Sel. Top. Appl. Earth Obs. Remote Sens.*, 13, 1467–1478, <https://doi.org/10.1109/JSTARS.2020.2983550>, 2020.
- Mann, H. B.: Nonparametric Tests Against Trend, *Econometrica*, 13, 245–259, <https://doi.org/10.2307/1907187>, 1945.
- Maskey, S., Uhlenbrook, S., and Ojha, S.: An analysis of snow cover changes in the Himalayan region using MODIS snow products and in-situ temperature data, *Clim. Change*, 108, 391–400, <https://doi.org/10.1007/s10584-011-0181-y>, 2011.
- 365 Matiu, M., Crespi, A., Bertoldi, G., Carmagnola, C. M., Marty, C., Morin, S., Schöner, W., Cat Berro, D., Chiogna, G., De Gregorio, L., Kotlarski, S., Majone, B., Resch, G., Terzago, S., Valt, M., Beozzo, W., Cianfarra, P., Gouttevin, I., Marcolini, G., Notarnicola, C., Petitta, M., Scherrer, S. C., Strasser, U., Winkler, M., Zebisch, M., Cicogna, A., Cremonini, R., Debernardi, A., Faletto, M., Gaddo, M., Giovannini, L., Mercalli, L., Soubeyroux, J.-M., Sušnik, A., Trenti, A., Urbani, S., and Weilguni, V.: Observed snow depth trends in the European Alps: 1971 to 2019, *The Cryosphere*, 15, 1343–1382, <https://doi.org/10.5194/tc-15-1343-2021>, 2021.
- 375 Melón-Nava, A.: Recent Patterns and Trends of Snow Cover (2000–2023) in the Cantabrian Mountains (Spain) from Satellite Imagery Using Google Earth Engine, *Remote Sens.*, 16, 3592, <https://doi.org/10.3390/rs16193592>, 2024.
- Notarnicola, C.: Hotspots of snow cover changes in global mountain regions over 2000–2018, *Remote Sens. Environ.*, 243, 111781, <https://doi.org/10.1016/j.rse.2020.111781>, 2020.
- 380 Ogliaro, L.: Frequenza, permanenza e ciclo della neve in Piemonte nel trentennio 1929 - 1958, *Istituto di Geografia Alpina*, 1971.
- Parajka, J. and Blöschl, G.: The value of MODIS snow cover data in validating and calibrating conceptual hydrologic models, *J. Hydrol.*, 358, 240–258, <https://doi.org/10.1016/j.jhydrol.2008.06.006>, 2008.
- Pinna, M.: La Durata del Manto Nevoso in Italia, in: *Atti della Tavola Rotonda sulla Geografia della Neve in Italia*, 1973.
- 385 Poussin, C., Peduzzi, P., and Giuliani, G.: Snow observation from space: An approach to improving snow cover detection using four decades of Landsat and Sentinel-2 imageries across Switzerland, *Sci. Remote Sens.*, 11, 100182, <https://doi.org/10.1016/j.srs.2024.100182>, 2025.
- Pratt, J. W. and Gibbons, J. D.: *Kolmogorov-Smirnov Two-Sample Tests*, in: *Concepts of Nonparametric Theory*, Springer New York, New York, NY, 318–344, [https://doi.org/10.1007/978-1-4612-5931-2\\_7](https://doi.org/10.1007/978-1-4612-5931-2_7), 1981.
- 390 Riggs, G., Hall, D., Vuyovich, C., and DiGirolamo, N.: Development of Snow Cover Frequency Maps from MODIS Snow Cover Products, *Remote Sens.*, 14, 5661, <https://doi.org/10.3390/rs14225661>, 2022.
- Saavedra, F. A., Kampf, S. K., Fassnacht, S. R., and Sibold, J. S.: Changes in Andes snow cover from MODIS data, 2000–2016, *The Cryosphere*, 12, 1027–1046, <https://doi.org/10.5194/tc-12-1027-2018>, 2018.
- Salomonson, V. V. and Appel, I.: Estimating fractional snow cover from MODIS using the normalized difference snow index, *Remote Sens. Environ.*, 89, 351–360, <https://doi.org/10.1016/j.rse.2003.10.016>, 2004.
- 395

- Sen, P. K.: Estimates of the Regression Coefficient Based on Kendall's Tau, *J. Am. Stat. Assoc.*, 63, 1379–1389, <https://doi.org/10.1080/01621459.1968.10480934>, 1968.
- Steiger, R., Scott, Daniel, Abegg, Bruno, Pons, Marc, and Aall, C.: A critical review of climate change risk for ski tourism, *Curr. Issues Tour.*, 22, 1343–1379, <https://doi.org/10.1080/13683500.2017.1410110>, 2019.
- 400 Sturm, M., Goldstein, M. A., and Parr, C.: Water and life from snow: A trillion dollar science question, *Water Resour. Res.*, 53, 3534–3544, <https://doi.org/10.1002/2017WR020840>, 2017.
- Trevisani, S., Skrypitsyna, T. N., and Florinsky, I. V.: Global digital elevation models for terrain morphology analysis in mountain environments: insights on Copernicus GLO-30 and ALOS AW3D30 for a large Alpine area, <https://doi.org/10.21203/rs.3.rs-2089787/v1>, 12 October 2022.
- 405 Tsai, W.-L., Leung, Y.-F., McHale, M. R., Floyd, M. F., and Reich, B. J.: Relationships between urban green land cover and human health at different spatial resolutions, *Urban Ecosyst.*, 22, 315–324, <https://doi.org/10.1007/s11252-018-0813-3>, 2019.